Coupling of SPH and Volume-of-Fluid

Markus Wicker, Niklas Bürkle, Rainer Koch, Hans-Jörg Bauer
Institute of Thermal Turbomachinery (ITS)
Karlsruhe Institute of Technology (KIT)
Karlsruhe, Germany
markus.wicker@kit.edu

I. Introduction

In multiphase flows, particularly those with chaotic interface fragmentation, SPH is commonly used due to its inherent interface capturing and associated high performance. Far from the interface however, the use of grid-based methods such as Volume-of-Fluid (VoF) methods is often preferable over SPH due to their higher maturity, e.g. in terms of variable resolution and turbulence modeling. Consequently, a coupled approach, in which an SPH domain, confined to the region of interface fragmentation, is embedded into a surrounding VoF domain, appears desirable.

Existing coupling approaches between SPH and Finite-Volume (FV) methods can be classified by their domain decomposition strategy: zonal (e.g. [1]–[4]), overlapping (e.g. [1], [2], [5]) and patched domains [6], [7]. In a zonal approach, the embedded domain is a subset of the surrounding domain which covers the entire computational domain. The embedded domain is used to impose its solution on the surrounding domain and is positioned to encompass the specific region of interest, e.g. a specific fluid, the interface region, or to capture shocks. In an overlapping approach, each domain encompasses regions exclusive to it. In the overlap however, both domains coexist, requiring either a blending or an iterative solution. A patched grid strategy, on the other hand features a discrete coupling interfaces connecting the disjoint domains.

Both the zonal and iterative overlapping approaches are not advisable in the context of atomization processes, as the expected increase of the already tremendous computational cost is prohibitive. A patched grid approach appears advantageous, as it enables a precise prescription of the coupling conditions between the domains. Of the existing patched grid coupling approaches [6], [7] between SPH and FV methods, the one proposed by Napoli et al. [6] also necessitates an iterative solution and is therefore unsuitable. The approach by Werdelmann et al. [7] is chosen as the foundation for the present work as is does not require an iterative solution and also possesses another conceptual advantage: most of the novel methodology is limited to the SPH domain. As a result, any existing FV package with a VoF solver can be used with minimal adaptations. In the present work, this approach is extended to couple SPH and VoF, enabling multiphase simulations.

II. Numerical methods

A. Smoothed Particle Hydrodynamics

In this work, an Arbitrary-Lagrangian-Eulerian (ALE), weakly-compressible SPH scheme similar to [7] is used. Particles are advected with a transport velocity $\vec{\tilde{u}} = \vec{u} + \vec{\delta u}$ consisting of the fluid velocity $\vec{u}$ and the shifting velocity $\vec{\delta u}$. The temporal derivatives of the density ρ and velocity of a particle i are derived as

$$\begin{aligned}\frac{d\rho_i}{dt} &= -\rho_i \sum_j V_j(\vec{u}_j - \vec{u}_i)\cdot\vec{\nabla}W_{ij} + \\ &\quad \vec{\delta u}_i \cdot \sum_{j\in\chi} V_j(\rho_j - \rho_i)\vec{\nabla}W_{ij} + \delta h_\sigma D_i^\rho \,, \qquad (1)\end{aligned}$$

$$\frac{d\vec{u}_i}{dt} = \vec{\delta u}_i \cdot \sum_j V_j(\vec{u}_j - \vec{u}_i)\otimes\vec{\nabla}W_{ij} + \vec{a}_i^{p,TIC} + \vec{a}_i^{\mu}\,. \qquad (2)$$

In this scheme, the mass of a particle m is kept constant within the domain and the particle volume is evaluated as $V = m/\rho$. The last term in (1) is the density diffusion term proposed by Ferrari et al. [8], scaled not with the 'geometrical' smoothing length h, but rather based on the kernel's standard deviation σ with $h_\sigma = 2\sigma$ [9], as well as the numerical parameter $\delta = 0.1$. The acceleration due to the pressure gradient $\vec{a}_i^p$ is computed using the tensile instability control by Sun et al. [10], while $\vec{a}_i^\mu$ denotes the accelerations due to viscous forces [11]. Of particular note are the second term on the RHS of (1) and the first in (2), which represent the ALE correction terms of particle density and velocity due to the shifting velocity. The density correction as well as the density diffusion is only computed over the neighbors j belonging the fluid χ of particle i.

The shifting velocity is evaluated from the particle concentration gradient [12], augmented by an additional repulsive interface force [13]:

$$\vec{\delta u} = -\varepsilon\frac{h_\sigma^2}{\delta t}\left(\sum_j V_j\vec{\nabla}W_{ij} + \varepsilon_{RIF}\sum_{j\notin\chi} V_j\vec{\nabla}W_{ij}\right). \qquad (3)$$

The parameter ε and ε_{RIF} are set to 0.5 and 0.01 throughout this work.

The system of equations is closed by the barotropic equation of state with the barotropic exponent γ, the speed of sound c

and the nominal density ρ_0:

$$p_i = \frac{\rho_{0,\chi} c_\chi^2}{\gamma_\chi} \left[\left(\frac{\rho_{i,\chi}}{\rho_{0,\chi}} \right)^{\gamma_\chi} + 1 \right] . \quad (4)$$

B. Volume-of-Fluid

As the proposed coupling approach is designed to require only minor modifications of an existing VoF CFD package, the employed VoF solver is derived from *compressibleInterIsoFoam*, a geometric VoF solver of *OpenFoam-v2212*, modified to employ the equation of state (4) and omitting the energy equation.

III. Coupling algorithm

The coupled interface is decomposed into boundary segments s with the area $A_s = dx^{d-1}$, in which dx is the mean particle distance and d the number of dimensions, which in this work is limited to 2. The flow variables, i.e. pressure p, velocity $\vec{u}$ and volume fraction α, are evaluated in the SPH domain through Shepard interpolation. Using this information, the coupling is enforced by prescribing matching Dirichlet boundary conditions to each domain. For the VoF domain this is trivial. For the SPH domain, Werdelmann et al. [7] have developed a novel permeable boundary approach, in which the SPH domain is extended by static 'ghost' particles which serve as interpolation points for the flow variables from the VoF domain. Their approach does not rely on a 'buffer' region but instead features an algorithm for the continuous mass flux across the boundary. This algorithm, detailed in [7], has to be adapted to enable coupling to VoF.

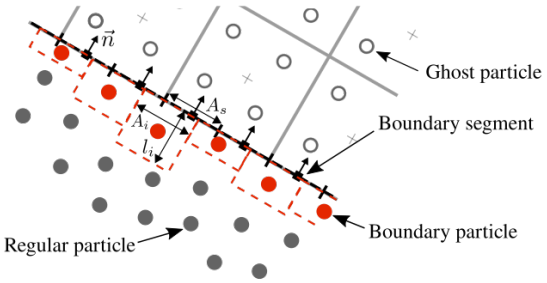

Fig. 1: Schematic representation of the coupling concept.

A. Mass Flux Algorithm

The total mass advected over a boundary segment s with the normal vector $\vec{n}$ in a time step $t \to t + \delta t$ is given by

$$\Delta m_s = \rho_s A_s \left(\vec{u}_s \cdot \vec{n}_s \right) \delta t . \quad (5)$$

In a VoF-type approach, the advected mass belonging to fluid χ can be expressed accordingly:

$$\Delta m_{s,\chi} = \alpha_{s,\chi} \rho_{s,\chi} A_s \left(\vec{u}_s \cdot \vec{n}_s \right) \delta t . \quad (6)$$

Together with (4), the relation between density, pressure and volume fraction is determined by

$$\rho_s = \alpha_s \rho_{s,1} + (1 - \alpha_s) \rho_{s,2} . \quad (7)$$

This mass flux is realized through a continuous increase or decrease of the mass of boundary particles based on some simple geometric considerations: Particles are considered to be cuboids, that are characterized by a square base with the area $A_i = A_s \left(\rho_{i,\chi} / \rho_{0,\chi} \right)^{\frac{1-d}{d}}$ parallel, and a height of $l_i = V_i / A_i$ perpendicular to the coupled interface. Under this assumption, the mass advected over the boundary can be derived from the positions $\vec{r}$ of particle i and boundary segment s and the transport velocity as

$$\delta m_i^* = -\rho_i A_i \left[\left(\vec{\tilde{u}} \cdot \vec{n} \right) \delta t - \left(\left(\vec{r}_s - \vec{r}_i \right) \cdot \vec{n} - \frac{l_i}{2} \right)^+ \right] . \quad (8)$$

The second term in the brackets is modified by the superscript $(\cdot)^+ = \max(0, \cdot)$ as it is only relevant when the particle is not in contact with the boundary prior to the advection. This predicted mass δm^* can associated with a boundary segment based on their geometric overlap $\omega = A_i \cap A_s$. As a result, the imbalance of the prescribed mass Δm and predicted mass δm^* can be evaluated for each boundary segment and each fluid. In order to optimize local and global mass conservation, this imbalance is compensated by imposing a corrective mass increment δm^{**} on the nearest eligible particle, or, if necessary, on a newly created particle. For details, especially with respect to the identification and creation of boundary particles, the reader is referred to [7].

B. Interface Handling

In vicinity of the fluid interface, the regular SPH particles are discretely associated with a single fluid, i.e. the fluid interface is discrete. In contrast, the volume fraction of VoF cells, and consequently ghost particles, as well as boundary segments is non-discrete, i.e. the fluid interface is continuous. As a result, straightforward application of the mass flux algorithm would lead to disturbances of the interface at the transition between domains. Hence, some additional considerations are necessary.

First, if for a boundary segment with $\alpha_{s,\chi} < 0.5$ the corrective mass increment of fluid χ δm_χ^{**} is non-zero, this increment is redistributed to the closest boundary segment in direction of the interface normal pointing into fluid χ for which $\alpha_{s,\chi} \geq 0.5$.

Second, a boundary particle can be 'trapped' within the other fluid if the interface is advected over the coupled boundary and the total advected mass is not an integer multiple of a nominal particle mass. To avoid adverse effects, these 'trapped' particles are identified and 'deactivated', i.e. they are no longer considered in the approximations in (1) and (2). Instead, these particles are only advected parallel to the coupled interface (denoted with the subscript $\|$) with the transport velocity $\vec{\tilde{u}} = \vec{u}_{s,\|} + \vec{\delta u}'_{\|}$. The shifting velocity $\vec{\delta u}'_{\|}$ is computed unilaterally, i.e. regular particles cause a shifting of the deactivated boundary particles, but not vice versa.

C. A Note on Temporal Discretization

In general, the two solvers use different time integration schemes with different stability regimes. While the SPH solver

performs explicit time integration, the VoF solver uses an implicit scheme. Consequently, while the state of the ghost particles $\vec{X}_g^{\nu}$ is simply interpolated at t_ν, the state of the boundary segments $\vec{X}_s^{\nu+1}$ has to be known ahead of the step $\nu \rightarrow \nu + 1$. Presently, this is handled through a consecutive solution of SPH and VoF equations with identical time steps. The development of a simultaneous solution algorithm with different discretization widths is part of the ongoing research.

IV. Validation

The proposed coupling method is validated through a Kelvin-Helmholtz benchmark case derived from [14] with a Reynolds number of $Re = 10^4$ and a Mach number of $Ma = 0.1$. The benchmark employs a periodic domain with $x \in [0, L]$ and $y \in [-L, L]$. Initially, fluid 2 occupies the region $y \in [-0.5L, 0.5L]$, while the rest of the domain is filled with fluid 1. The coupled boundaries are positioned at $y_1 = 0.25L$ and $y_2 = 0.75L$, resulting in an intersection with the fluid interface in the non-linear regime of the instability growth.

The SPH particles are initialized on a Cartesian lattice with a spacing of $dx_1 = L/600$. A quintic B-spline kernel with a kernel radius of $H = 3dx$ is employed. The VoF domain is discretized by a Cartesian grid, with the cell size Δx set to match the kernel radius H. In addition to the coupled simulation, references results with both VoF and SPH are obtained in simulations matching the resolutions from the coupled setup. Simulations are performed until $t = 4$, capturing both the linear and non-linear regime of the instability growth.

The final fluid distribution is depicted in Fig. 2. Evidently,

Fig. 2: Fluid distribution in the region $x, y \in [0, L]$ from the VoF, SPH and Coupled SPH-VoF simulations at $t = 4$. The lighter and darker blue represent fluid 1 and 2 respectively.

the instability is captured well by all 3 simulations, with almost identical results between the coupled and SPH simulations and only minor differences to the VoF results.

In addition to the fluid distribution, the amplitude of the seeded instability mode $k = 2\pi L$ [15] is displayed in Fig. 3. Again, it is clear, that the results of the coupled case match the reference results very well.

Acknowledgment

The authors acknowledge funding by the German Federal Ministry for Economic Affairs and Climate Action (BMWK) within the framework of research program Luftfahrtforschungsprogramm 6 (Funding No. 20D2102B).

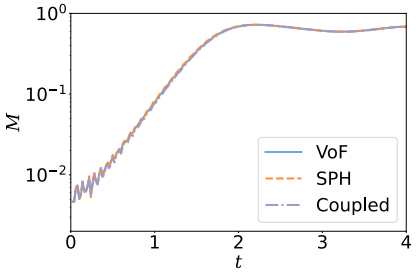

Fig. 3: Amplitiude M of theinstability mode $k = 2\pi L$ from the VoF, SPH and Coupled SPH-VoF simulations for $t \in [0, 4]$.

References

[1] M. Neuhauser, "Development of a coupled SPH-ALE/Finite Volume method for the simulation of transient flows in hydraulic machines," phdthesis, Ecole Centrale de Lyon, Dec. 2014.

[2] A. Di Mascio, S. Marrone, A. Colagrossi, L. Chiron, and D. Le Touzé, "SPH–FV coupling algorithm for solving multi-scale three-dimensional free-surface flows," *Applied Ocean Research*, vol. 115, p. 102846, Oct. 2021.

[3] Y. Xu, G. Yang, and D. Hu, "A three-dimensional ISPH-FVM coupling method for simulation of bubble rising in viscous stagnant liquid," *Ocean Engineering*, vol. 278, p. 114497, Jun. 2023.

[4] C. Myers, T. Palmer, and C. Palmer, "A hybrid Finite Volume-Smoothed Particle Hydrodynamics approach for shock capturing applications," *Computer Methods in Applied Mechanics and Engineering*, vol. 417, p. 116412, Dec. 2023.

[5] S. Marrone, A. Di Mascio, and D. Le Touzé, "Coupling of Smoothed Particle Hydrodynamics with Finite Volume method for free-surface flows," *Journal of Computational Physics*, vol. 310, pp. 161–180, Apr. 2016.

[6] E. Napoli, M. Marchis, C. Gianguzzi, B. Milici, and A. Monteleone, "A coupled Finite Volume–Smoothed Particle Hydrodynamics method for incompressible flows," *Computer Methods in Applied Mechanics and Engineering*, vol. 310, pp. 674–693, 2016.

[7] B. Werdelmann, R. Koch, W. Krebs, and H.-J. Bauer, "An approach for permeable boundary conditions in SPH," *Journal of Computational Physics*, vol. 444, p. 110562, 2021.

[8] A. Ferrari, M. Dumbser, E. F. Toro, and A. Armanini, "A new 3D parallel SPH scheme for free surface flows," *Computers & Fluids*, vol. 38, no. 6, pp. 1203–1217, 2009.

[9] W. Dehnen and H. Aly, "Improving convergence in smoothed particle hydrodynamics simulations without pairing instability," *Mon. Not. R. Astron. Soc.*, vol. 425, no. 2, pp. 1068–1082, 2012.

[10] P. N. Sun, A. Colagrossi, S. Marrone, M. Antuono, and A. M. Zhang, "Multi-resolution Delta-plus-SPH with tensile instability control: Towards high Reynolds number flows," *Computer Physics Communications*, vol. 224, pp. 63–80, Mar. 2018.

[11] K. Szewc, J. Pozorski, and J.-P. Minier, "Analysis of the incompressibility constraint in the smoothed particle hydrodynamics method," *International Journal for Numerical Methods in Engineering*, vol. 92, no. 4, pp. 343–369, 2012.

[12] S. J. Lind, R. Xu, P. K. Stansby, and B. D. Rogers, "Incompressible smoothed particle hydrodynamics for free-surface flows: A generalised diffusion-based algorithm for stability and validations for impulsive flows and propagating waves," *Journal of Computational Physics*, vol. 231, no. 4, pp. 1499–1523, Feb. 2012.

[13] N. Grenier, M. Antuono, A. Colagrossi, D. Le Touzé, and B. Alessandrini, "An Hamiltonian interface SPH formulation for multi-fluid and free surface flows," *Journal of Computational Physics*, vol. 228, no. 22, pp. 8380–8393, 2009.

[14] D. Lecoanet, M. McCourt, E. Quataert, K. J. Burns, G. M. Vasil, J. S. Oishi, B. P. Brown, J. M. Stone, and R. M. O'Leary, "A validated non-linear Kelvin–Helmholtz benchmark for numerical hydrodynamics," *Mon. Not. R. Astron. Soc.*, vol. 455, no. 4, pp. 4274–4288, 2016.

[15] T. S. Tricco, "The kelvin–helmholtz instability and smoothed particle hydrodynamics," *Monthly Notices of the Royal Astronomical Society*, vol. 488, no. 4, pp. 5210–5224, 2019.